Splitting a C–O bond in dialkylethers with bis(1,2,4-tri-*tert*-butylcyclopentadienyl)cerium hydride does not occur by a σ-bond metathesis pathway: a combined experimental and DFT computational study†

Evan L. Werkema,[a] Ahmed Yahia,[bc] Laurent Maron,*[b] Odile Eisenstein*[d] and Richard A. Andersen*[a]

Received (in Montpellier, France) 6th April 2010, Accepted 17th May 2010
DOI: 10.1039/c0nj00261e

The addition of diethylether to $[1,2,4(Me_3C)_3C_5H_2]_2CeH$, abbreviated Cp'_2CeH, gives Cp'_2CeOEt and ethane. Similarly, di-n-propyl- or di-n-butylether gives Cp'_2Ce(O-n-Pr) and propane or Cp'_2Ce(O-n-Bu) and butane, respectively. Using Cp'_2CeD, the propane and butane contain deuterium predominantly in their methyl groups. Mechanisms, formulated on the basis of DFT computational studies, show that the reactions begin by an α- or β-CH activation with comparable activation barriers, but only the β-CH activation intermediate evolves into the alkoxide product and an olefin. The olefin then inserts into the Ce–H bond forming the alkyl derivative, Cp'_2CeR, which eliminates alkane. The α-CH activation intermediate is in equilibrium with the starting reagents, Cp'_2CeH and the ether, which accounts for the deuterium label in the methyl groups of the alkane. The one-step σ-bond metathesis mechanism has a much higher activation barrier than either of the two-step mechanisms.

Introduction

It has been shown recently that monomeric metallocenecerium hydride $[1,2,4(Me_3C)_3C_5H_2]_2CeH$, Cp'_2CeH (shown in Scheme 1), reacts with methyl halides, forming the seemingly straightforward H for X exchange products Cp'_2CeX and methane (eqn (1)).

$$Cp'_2CeH + CH_3X \rightarrow Cp'_2CeX + CH_4 \qquad (1)$$

The mechanism of the exchange reaction does not proceed by way of a direct σ-bond metathesis transition state, since experimental and computational studies showed that the reactions proceed by a two-step mechanism, forming the products shown in eqn (1). The first step is a CH bond activation generating a carbenoid intermediate, $Cp'_2Ce(\eta^2\text{-}CH_2X)$, and H_2, followed by a second step that involves trapping of CH_2 by H_2.[1,2] No intermediates were observed in the reactions of Cp'_2CeH by NMR spectroscopy. When the metallacycle $Cp'[(Me_3C)_2C_5H_2C(CH_3)_2CH_2]Ce$ (shown in Scheme 1) is used, *i.e.*, when H_2 is not present, NMR evidence has been obtained of an intermediate, $Cp'_2Ce(\eta^2\text{-}CH_2X)$ (shown in Scheme 1), where X = Cl, Br or I (eqn (2)).

$$Cp'[(Me_3C)_2C_5H_2C(CH_3)_2CH_2]Ce + CH_3X \rightarrow Cp'_2Ce(\eta^2\text{-}CH_2X) \rightarrow Cp'_2CeX + \text{“}CH_2\text{”} \qquad (2)$$

When X = OMe, $Cp'_2Ce(\eta^2\text{-}CH_2OMe)$ was isolated, even in presence of H_2, and the methoxymethyl derivative slowly formed Cp'_2CeOMe.[2] The net reaction of Me_2O with Cp'_2CeH that gives Cp'_2CeOMe and CH_4 is analogous to the net reaction between $(C_5Me_5)_2MH$ and Et_2O, which gives the ethoxide $(C_5Me_5)_2MOEt$ and ethane. The reaction was first reported by Watson[3] for M = Lu, who showed that when Et_2O-d_{10} was used, the ethane isotopologue was CHD_2CD_3 and no ethene was observed. This result lead to the suggestion that ethane was formed by direct attack of the hydride on the carbon α to the oxygen. This statement clearly implicates a four-center mechanism for the reaction, although the term σ-bond metathesis, coined by Bercaw and co-workers, was not in the literature at the time of Watson's initial studies.[4] The mechanism of a σ-bond metathesis reaction, *i.e.*, a net reaction in which the σ bonds exchange partners, is a concerted process that occurs in a single step, in which the four participating atoms or groups have a kite-shaped transition state. In this article, the term σ-bond metathesis transition state and mechanism of a σ-bond metathesis reaction refer to the same physical mechanism or pathway. Later, the σ-bond metathesis terminology was used by Teuben and co-workers to describe analogous reactions between $(C_5Me_5)_2MH$, M = Y, La, Ce and Et_2O.[5] A similar pathway was mentioned for the formation of $(C_5Me_5)_2SmOEt$ from $(C_5Me_5)_2SmH$ and Et_2O.[6]

Computational studies on the reaction between $(C_5H_5)_2CeH$ and Me_2O showed that the activation barrier for a σ-bond

[a] *Department of Chemistry and Chemical Sciences Division of Lawrence Berkeley National Laboratory, University of California, Berkeley, California 94720-1460, USA*
[b] *LPCNO, Université de Toulouse, INSA, UPS, LPCNO, 135 avenue de Rangueil, F-31077 Toulouse, France and CNRS, LPCNO, F-31077 Toulouse, France*
[c] *ICSM UM5257, CEA-CNRS-UM2, Site de Marcoule, BP17171, 30207 Bagnols-sur-Cèze, France*
[d] *Institut Charles Gerhardt, Université Montpellier 2, CNRS 5253, cc 1501, Place E. Bataillon, F-34095 Montpellier, France*
† Electronic supporting information (ESI) available: Coordinates, energies *E* and free energies *G* in a.u. of all calculated extrema. See DOI: 10.1039/c0nj00261e

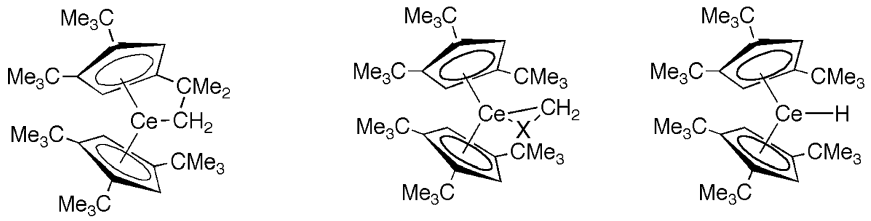

$Cp'[(Me_3C)_2C_5H_2C(CH_3)_2CH_2]Ce$ $Cp'_2Ce(\eta^2\text{-}CH_2X)$ Cp'_2CeH

Scheme 1

metathesis transition state is higher than that of the two-step pathway by about 4 kcal mol^{-1}; a deduction that is consistent with the experimental studies on Cp'_2CeH.[2] Thus, a mechanistic quandary is apparent, since if the σ-bond metathesis transition state is a high energy pathway for Me_2O, then it is presumably also high for Et_2O. If this conjecture is correct, then the mechanism for the formation of Cp_2CeOEt and ethane could proceed by either (i) σ-bond metathesis (ii) α- or perhaps by (iii) β-CH activation, where the α- and β-CH notation refers to the CH bonds α or β to the oxygen atom of the ether, respectively.

In this article, we show that the reaction between Cp'_2CeH and symmetrical dialkylethers RCH_2CH_2OR' (R = H, Me, Et; R′ = CH_2CH_2R) does not proceed by way of the single step σ-bond metathesis transition state but by way of a two-step process, the first of which is a β-CH activation, followed by an alkoxy transfer step with olefin elimination. In a subsequent reaction, the olefin inserts into the Ce–H bond, forming an alkyl complex, which reacts with H_2, forming an alkane and Cp'_2CeH, or alkane elimination, forming the metallacycle and alkane. Thus, the net C–O bond cleavage reaction is as shown in eqn (3).

$$Cp'_2CeH + RCH_2CH_2OR' \rightarrow Cp'_2CeOR' + CH_3CH_2R \quad (3)$$

Results

(1) Experimental studies

The reactions between Cp'_2CeH and the dialkyl ethers were conducted in NMR tubes and the course of the reaction monitored by ^1H NMR spectroscopy. The reactions were slow, as shown by the disappearance of the resonances due to Cp'_2CeH and the appearance of resonances due to Cp'_2CeOR' and CH_3CH_2R (eqn (3)). For example, the ratio of Cp'_2CeH to Cp'_2CeOEt was approximately 1 : 4 after 36 d at 20 °C. The ratio of Cp'_2CeH to Cp'_2CeO-n-Pr or Cp'_2CeO-n-Bu was approximately 1 : 2 after 101 d at 60 °C and the relative rates were Et ≫ *n*-Pr ≈ *n*-Bu. The alkoxide derivatives were isolated and characterized as outlined in the Experimental section. In contrast, the reaction between Cp'_2CeH and Me_2O rapidly formed $Cp'_2Ce(\eta^2\text{-}CH_2OMe)$ and H_2, and the former slowly evolved into the methoxide Cp'_2CeOMe.[2] When R′ is Et, n-Pr and n-Bu, no resonances due to a hypothetical α-CH activation intermediate $Cp'_2Ce(C(H)(CH_2R)OR')$ were detected, which implies that if α-CH activation occurred, the intermediates went straight to the alkoxide products, or the net reactions followed a different pathway, such as β-CH activation or the direct elimination of CH_3CH_2R.

An experimental distinction between a direct alkane elimination or an α- or β-CH activation preceding alkane formation was possible using deuterium labelled $(Cp'\text{-}d_{27})_2CeD$ and n-Pr_2O or n-Bu_2O, since these reactions are clean but slow, and the deuterium incorporated into the various sites of the ethers and hydrocarbon could be monitored over time. For example, monitoring the reaction between $(Cp'\text{-}d_{27})_2CeD$ and n-Bu_2O in C_6D_6 by ^1H, ^2H, and $^{13}C\{^1H\}$ NMR spectroscopy showed that deuterons were incorporated into the α and δ sites in non-statistical amounts. After 147 d at 60 °C, when the conversion of $(Cp'\text{-}d_{27})_2CeD$ to $(Cp'\text{-}d_{27})_2CeO$-n-Bu was complete, the relative distribution of the deuterons into the excess $(n\text{-}Bu)_2O$ was α ≫ δ in the ^2H and $^{13}C\{^1H\}$ NMR spectra. Using the integrated intensities of the two resonances in the ^2H NMR spectrum yielded an α : δ ratio of 10 : 1. This result shows that H/D exchange accumulated deuterons into the α-site, which implies that the α-CH activation is reversible. No deuterium was detected in the β or γ sites of $(n\text{-}Bu)_2O$, but the butane produced by the reaction contained deuterium in both the primary and secondary sites in a ratio of 5 : 1. This result implies that β-CH activation is productive in splitting the C–O bond to generate the alkoxide and a terminal alkene, which is hydrogenated to the alkane by Cp'_2CeH. A similar conclusion was reached from an analysis of the reaction between $(Cp'\text{-}d_{27})_2CeD$ and n-Pr_2O (see the Experimental section for details). These studies show that the mechanism for ether cleavage depends upon whether the ethers have β-hydrogens. The different reaction mechanisms are explored by the computational studies outlined in the following section.

(2) Computational studies

The DFT(B3PW91) calculations utilized the methodology described in previous studies.[1,2,7] As before, Cp′ was modeled by Cp (C_5H_5) due to the prohibitive complexity of calculations involving Cp′ metallocenes. While a substitution alters the geometric and steric environment of the metal center, and consequently the absolute values of the calculated energies, the reactivity trends predicted computationally for Cp complexes for small molecules generally agree with those observed experimentally for the analogous Cp′ complexes. The modeling should likewise be valid for the ether reactions presented in this paper.

The free energy profiles for the reaction of Cp_2CeH, abbreviated as [Ce]H, with Et_2O, n-Pr_2O and n-Bu_2O are

shown in Fig. 1. The Gibbs free energy, G, of all extrema are given relative to the separated reactants [Ce]H and ether. The activation barrier is defined as the difference in Gibbs free energy between a transition state and its associated reactants.

The one-step σ-bond metathesis reaction was calculated for Et_2O. The transition state has a Gibbs free energy of 44.2 kcal mol^{-1}. This is close to the 43.5 kcal mol^{-1} value obtained for Me_2O, and higher than those obtained for CH_3X when X equals halide.[2] These two values strongly indicate that the direct H for OR exchange is not the mechanism for the formation of [Ce]OEt. This path was not explored for the n-Pr_2O and n-Bu_2O reactions. Alternative mechanistic pathways are explored next.

The α-CH activation starts by the formation of an ether adduct whose free energy of −4.6 kcal mol^{-1} slightly beats the loss in entropy, and the formation of the adducts is exoergic. The transition state for the α-CH bond activation has a free energy of 14.2 kcal mol^{-1} relative to separated [Ce]H and ether, very close to the value of 13.8 kcal mol^{-1} obtained for Me_2O. The resulting 3-membered ring [Ce](η^2-CH(Me)OEt) has a Gibbs free energy of −0.5 kcal mol^{-1}, essentially equal to that of −0.9 kcal mol^{-1} for [Ce](η^2-CH_2-OMe). The free energy of the transition state for the insertion of $CH(CH_3)$ into H_2 is 41.1 kcal mol^{-1} relative to the energy reference, slightly higher than that of the 37.9 kcal mol^{-1} calculated for [Ce](η^2-CH_2OMe). The trapping reaction of CH_2 by H_2 was shown previously, in the case of [Ce](η^2-CH_2F), [Ce](η^2-CHF_2) and [Ce](η^2-CF_3) with H_2, to be largely controlled by the electrophilicity of the carbene that is formed upon cleavage of the C–F and Ce–C bonds.[1] A similar effect is apparent in this case, even though the π-electron donating ability of the methyl group in CH(Me) is less than that of F. The high activation barrier of the trapping reaction means that the α-CH activation pathway is not productive. Since the activation barrier for the α-CH activation step is low, and since the ether adduct and the [Ce](η^2-CH(Me)OEt) intermediate are isoergic, an equilibrium exists between these two molecules, which accounts for the accumulation of deuterium in the α-sites of the dialkylethers.

The β-CH activation pathway starts from an adduct at −2.6 kcal mol^{-1}, similar to that for the α-CH activation; the adducts differ only in the conformation of the two Et groups. From this adduct, the transition state for β-CH activation has a Gibbs free energy of 15.1 kcal mol^{-1} relative to the energy reference, only slightly higher than that for the α-CH activation. From this transition state, the four-membered CeOCC ring,

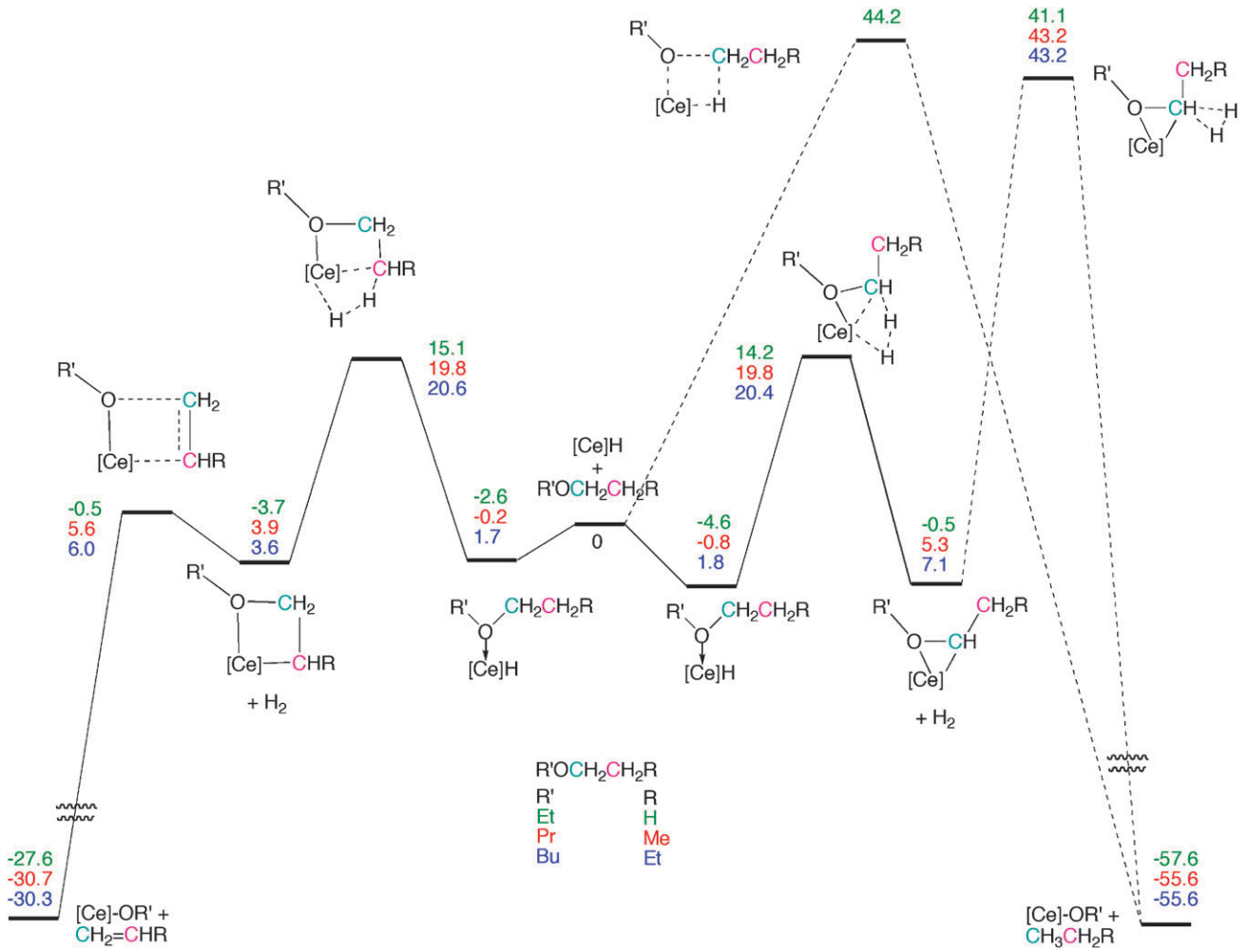

Fig. 1 Gibbs free energy profiles (kcal mol^{-1}) for the reaction pathways of [Ce]H with Et_2O, n-Pr_2O and n-Bu_2O. On the right, σ-bond metathesis and α-CH activation. On the left, β-CH activation.

with an energy of −3.7 kcal mol^{-1}, is slightly more stable than the three-membered CeOC ring originating from the α-CH activation, reflecting the decreased ring strain in the four-membered ring. The four-membered ring metallacycle [Ce](η^2-CH_2-CH_2-OEt) evolves into the products CH_2=CH_2 and [Ce]OEt with a low activation energy of −3.2 kcal mol^{-1} relative to the four-membered ring intermediate. The favorable free energy of reaction of −27.6 kcal mol^{-1} is the result of the formation of a strong Ce–OR bond.

[Ce]OEt is an observed product but ethene is not, since only the saturated alkane, ethane in this case, is observed. Several pathways are possible for the conversion of ethylene to ethane: (i) ethylene can insert into the Ce–H bond and the resulting [Ce]Et undergo hydrogenolysis with H_2, forming [Ce]H and ethane, or (ii) the ethyl complex can eliminate ethane, forming the metallacycle, since the isolated Cp′$_2$CeCH$_2$Ph reacts with H_2 to form Cp′$_2$CeH and toluene, and forms the metallacycle and toluene in the absence of H_2. Both pathways are reasonable ones for the formation of alkanes from the hypothetical alkyl Cp′$_2$CeCH$_2$CH$_2$R.[8] Insertion of an olefin into a metal hydride bond for d^0 metal complexes has been extensively studied by computations as the initial step in polymerization reactions;[9] in all cases, the activation barrier was low, which accounts for the fact that no transition state for ethylene insertion into the Ce–H bond was located. Given the large body of computational studies that show the low activation barriers for olefin insertion, the formation of an alkane product was not explored computationally for Cp_2CeH and an olefin in this article.

The structures of the intermediates and transition states for these two reactions are not surprising (Fig. 2 and Fig. 3). The geometry for α-CH activation with Et_2O is similar to that for Me_2O, the main characteristic being the open $C_\alpha\cdots H\cdots H$ angle of 171°. The geometry for β-CH activation has the same $C_\beta\cdots H\cdots H$ angle of 171° (Fig. 2). The slightly higher energy of the transition state for β-CH activation compared to that of α-CH activation is, in part, due to the eclipsed orientation of the ethyl group in the transition state.

The three-membered CeOC ring in [Ce](η^2-CH(Me)OEt) has similar features (Ce–C = 2.552 Å; Ce–O = 2.450; C–O = 1.464 Å) to those calculated for [Ce](η^2-CH_2OMe) (Ce–C = 2.510 Å, Ce–O = 2.445 Å; C–O = 1.461 Å).[2] The marginal lengthening of the Ce–C bond in [Ce](η^2-CH(Me)OEt) is due to the steric effect of the ethyl substituent. The four-membered

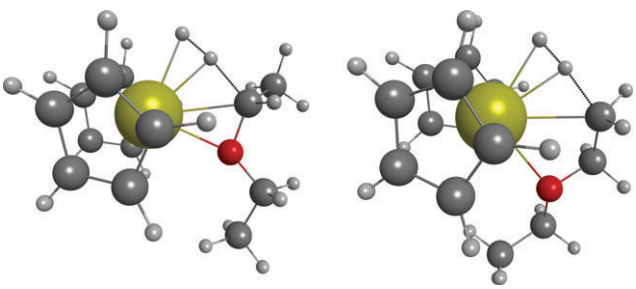

Fig. 2 Optimized structures of the transition states for, left, the α-CH activation and, right, the β-CH activation. The color codes are yellow for cerium, red for oxygen, dark grey for carbon and light grey for hydrogen.

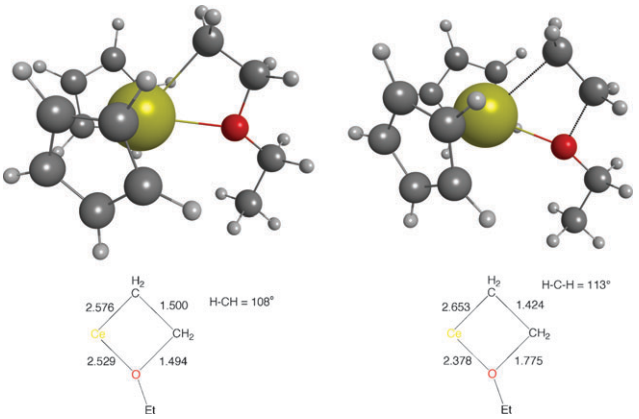

Fig. 3 Optimized structures for (a) the four-membered ring [Ce](η^2-CHRCH$_2$OR′) (R = H, R′ = CH_2CH_3) and (b) the associated transition states for the ejection of CHR=CH_2. The geometrical features are similar for R = Me and Et. The selected distances are in Å and angles in degrees. The color codes are yellow for cerium, red for oxygen, dark grey for carbon and light grey for hydrogen.

CeOCC ring resulting from β-CH activation is planar (Fig. 3). The C–C bond length of 1.500 Å is close to the value for a C–C single bond (1.54 Å) and the Ce–C bond of 2.576 Å is of identical length to that of the 2.577(4) Å observed in Cp′$_2$CeCH$_2$Ph;[8] the elongated intra-ring C–O distance of 1.494 Å is significantly longer than the *exo*-ring C–O(Et) distance of 1.42 Å. The calculated Ce–O bond length is 2.529 Å. Comparison with an experimental value is not available since only the structure of the three-membered ring [Ce](η^2-CH_2OMe) is known. The transition state for ethene elimination shows an elongation of the "long" C–O bond to a distance of 1.775 Å, stretching the Ce–C bond to 2.653 Å, while shortening the C–C distance to 1.424 Å and also the Ce–O bond to 2.378 Å as it forms a Ce–O bond of 2.163 Å in [Ce]OEt (Fig. 3). The four-membered ring remains planar at the transition state and the ethylene is essentially planar, since the angles at carbon sum to 348.5°.

The reaction pathways for the reactions of n-Pr_2O and n-Bu_2O with [Ce]H are similar to those obtained for Et_2O, but all intermediates and transition states are higher in energy by 5 to 7 kcal mol^{-1} relative Et_2O. Since the free energy profiles for n-Pr_2O and n-Bu_2O are close together, the substituents closer to the oxygen atom have a larger influence on the energies than those further away, and the relative free energy profiles are in good agreement with the relative rates observed as one proceeds from Et_2O to n-Pr_2O to n-Bu_2O in the experimental reaction.

Discussion

The net reaction between Cp′$_2$CeH and dialkylethers results in the alkoxy for H exchange illustrated in eqn (3). Computational studies show that of the three possible mechanisms considered, the direct exchange through a σ-bond metathesis transition state has the highest activation barrier. Lower energy processes that involve the initial α- or β-CH activation, forming three and four-membered ring intermediates, respectively, are comparable in energy. These relative

energies should not be significantly changed with Cp′ ligands instead of Cp, and in particular, the σ-bond metathesis pathway should remain the pathway with the highest energy barrier. The essentially equivalent activation barriers for α- and β-CH activation show that the acidity of the CH bonds is not the only factor that determines the selectivity, but that the ring strain at the transition state is also important. These intermediates evolve into products by ejection of a carbene or an olefin, respectively, and the activation barrier for the former transformation is substantially higher than that for the latter. Thus, the α-CH activation intermediate does not lead to the product, whereas the β-CH activation intermediate leads to C–O bond cleavage. The relative activation barriers identified in the computational studies of the potential energy surfaces for the three pathways considered are consistent with the experimental observations, which show that (i) the rates of the reactions are slow, (ii) deuterium from Cp'_2CeD is preferentially distributed into the α-CH sites of the dialkylethers and the terminal methyl groups in the alkanes, and (iii) no intermediates build up in sufficient concentration to be detected by ^1H NMR spectroscopy. The eliminated olefin is postulated to be trapped by Cp'_2CeH, forming the alkyl that rapidly undergoes hydrogenolysis or/and alkane elimination, forming the metallacycle, which is trapped by H_2, reforming Cp'_2CeH. The principle that emerges from these studies is that even though an alkane, rather than an olefin, is the product observed when the ether contains β-hydrogens, the reaction proceeds by way of olefin elimination, and the olefin is converted to the alkane rapidly. This accounts for the lack of detectable intermediates, in contrast to, for example, the isolation of $Cp'_2Ce(\eta^2\text{-}CH_2OMe)$ when Me_2O is used.[2] Thus, the C–O cleavage reaction in dialkylethers leads to the net alkoxy for hydrogen exchange, and the mechanism depends upon the nature of the alkyl group.

The reactions of Cp'_2CeH with dialkylethers described in this and an earlier article[2] have a parallel with reactions of alkyllithium reagents with Me_2O and Et_2O. Ziegler showed sixty years ago that Me_2O and RLi generate a "methylene carbenoid", which evolves into LiOMe and $LiCH_2R$.[10] Thus, the organolithium reagent traps the methylene fragment, a net reaction that is somewhat similar to the reaction of Cp'_2CeH and Me_2O.[2] Later, it was shown that RLi reagents react with appropriately labelled diethylether to give lithium alkoxides and an olefin; the distribution of deuterium shows that the major pathway is β-CH abstraction, though a small fraction is formed by α-CH abstraction, similar to the reactions described in this article.[11] The ether cleavage reactions have considerable synthetic utility and are the subject of reviews.[12]

The choice between α- and β-CH activation pathways in ethers carries over to amines. The metalation reaction of $Me_2NCH_2CH_2NMe_2$ with $LiCMe_3$ gives $Me_2NCH_2CH_2N(Me)(CH_2Li)$ and Me_3CH, but with $Et_2NCH_2CH_2NEt_2$ the products are $Et_2NCH_2CH_2N(Et)(Li)$, ethylene and Me_3CH.[13] The computational studies outlined in ref. 13 also show that the β-CH activation barrier is about 5 kcal mol^{-1} lower than that for α-CH activation. In d-transition metal chemistry, the addition of, for example, diethylether to a zirconium metallocene gives [Zr](H)(OEt) and [Zr](C_2H_4), where [Zr] is a bis(substituted indenyl) metallocene fragment. The suggested mechanism involves an equilibrium between the α- and β-CH activation intermediates, and the latter evolves into the two isolated products.[14] It is noteworthy that the four-membered ring $MOCH_2CH_2$ intermediate advocated in this article may be important in the exchange of β-CHs with deuterons in $Ta(OEt)_5$ and EtOD, and related alcohols.[15]

Conclusion

The experimental reaction between Cp'_2CeH and the dialkylethers RCH_2CH_2OR', where R = H, Me, Et; R′ = CH_2CH_2R) gives Cp'_2CeOR' and R′H. The DFT calculations of the potential energy surfaces for each ether with $(C_5H_5)_2CeH$ shows that a one-step OR′ for H exchange pathway has a higher activation barrier than two different two-step pathways that begin by α- or β-CH activation, forming $Cp_2Ce[\eta^2\text{-}CH(CH_2R)OR']$ and $Cp_2Ce[\eta^2\text{-}CH(R)CH_2OR']$, respectively, both of which have comparable activation barriers but only the latter intermediate yields the alkoxide product with evolution of an olefin. The mechanistic pattern that emerges from the combined experimental and computational studies is that β-CH activation followed by olefin elimination has a lower activation barrier than α-CH activation followed by carbene elimination. This reactivity pattern seems to be general for metals that cannot undergo oxidative addition–reductive elimination cycles.

Experimental section

General

All manipulations were performed under an inert atmosphere using standard Schlenk and dry box techniques. All solvents and ethers were dried and distilled from sodium or sodium benzophenone ketyl. Alkoxytrimethylsilane reagents were distilled under nitrogen and vacuum transferred into greaseless flasks. NMR spectra were recorded on Bruker AV-300, AV-400 or AV-600 spectrometers at 20 °C in the solvent specified. J-Young NMR tubes or sealed NMR tubes were used for all NMR tube experiments. Electron impact mass spectrometry and elemental analyses were performed by the microanalytical facility at the University of California, Berkeley. The abbreviation Cp′ is used for the 1,2,4-tri-*tert*-butylcyclopentadienyl ligand. GCMS analysis was performed on an HP6890 GC system with a J&W DB-XLB universal non-polar column attached to an HP5973 mass selective detector.

Syntheses

Cp'_2CeOEt. Cp'_2CeH[16] (0.55g, 0.90 mmol) was dissolved in pentane (10 mL) and ethoxytrimethylsilane (0.2 mL, 1.3 mmol) was added *via* syringe. The purple solution turned red over 10 min. After 30 min, the sample was taken to dryness and the glassy red solid was added to glass ampoules, sealed under vacuum and sublimed at 185 °C. The resulting deep red plates and microcrystals were sealed under vacuum in a fresh ampoule and sublimed again at 185 °C. Yield: 150 mg (0.23 mmol, 25%). MP = 317–319 °C. ^1H NMR (C_6D_6): δ 32.88 (2H, $\nu_{1/2}$ = 30 Hz), 24.40 (4H, $\nu_{1/2}$ = 60 Hz), 11.06 (3H, $\nu_{1/2}$ = 15 Hz), −1.69 (36H, $\nu_{1/2}$ = 40 Hz), −11.11

(18H, $\nu_{1/2}$ = 25 Hz). MS $(M)^+$ *m/z* (calc., found) 651 (100, 100), 652 (40, 53), 653 (20, 32), 654 (6, 15), 655 (1, 3). Anal. calc. for $C_{36}H_{63}CeO$: C, 66.32; H, 9.74. Found C, 66.29; H, 9.64%.

Cp′$_2$CeO-n-Pr. Cp′$_2$CeH (0.42g, 0.69 mmol) was dissolved in pentane (10 mL) and n-propoxytrimethylsilane (0.15 mL, 0.87 mmol) was added *via* syringe. The purple solution turned red over 10 min. After 30 min, the sample was taken to dryness and the glassy red solid was added to glass ampoules, sealed under vacuum and sublimed at 185 °C. The resulting deep red microcrystals were sealed under vacuum in a fresh ampoule and sublimed again at 185 °C. Yield: 130 mg (0.19 mmol, 28%). MP = 315–318 °C. ^{1}H NMR (C_6D_6): δ 33.25 (2H, $\nu_{1/2}$ = 30 Hz), 24.74 (4H, $\nu_{1/2}$ = 70 Hz), 11.66 (2H, $\nu_{1/2}$ = 15 Hz), 5.85 (3H, $\nu_{1/2}$ = 15 Hz), −1.48 (36H, $\nu_{1/2}$ = 80 Hz), −11.73 (18H, $\nu_{1/2}$ = 25 Hz). MS $(M)^+$ *m/z* (calc., found) 665 (100, 100), 666 (41, 52), 667 (21, 30), 668 (6, 7). Anal. calc. for $C_{37}H_{65}CeO$: C, 66.72; H, 9.84. Found C, 66.89; H, 10.12%.

Cp′$_2$CeO-n-Bu. n-Butoxytrimethylsilane was prepared from n-butyl alcohol, chlorotrimethylsilane and triethylamine following published procedures.[17] Cp′$_2$CeH (0.38 g, 0.63 mmol) was dissolved in pentane (10 mL) and n-butoxytrimethylsilane (0.16 mL, 0.85 mmol) was added *via* syringe. The purple solution turned red over 10 min. After 30 min, the sample was taken to dryness, warmed gently under a dynamic vacuum to remove excess n-butoxytrimethylsilane and the glassy red solid added to glass ampoules, sealed under vacuum and sublimed at 185 °C. The resulting gummy, deep red solid was sealed under vacuum in a fresh ampoule and sublimed again at 185 °C. Yield: 60 mg (0.088 mmol, 14%). ^{1}H NMR (C_6D_6): δ 33.43 (2H, $\nu_{1/2}$ = 40 Hz), 24.75 (4H, $\nu_{1/2}$ = 70 Hz), 11.71 (2H, $\nu_{1/2}$ = 25 Hz), 6.63 (2H, $\nu_{1/2}$ = 25 Hz), 3.62 (3H, t, J = 8 Hz), −1.40 (36H, $\nu_{1/2}$ = 85 Hz), −11.80 (18H, $\nu_{1/2}$ = 30 Hz). MS $(M)^+$ *m/z* (calc., found) 679 (100, 100), 680 (42, 56), 681 (21, 35), 682 (6, 15). Anal. calc. for $C_{37}H_{65}CeO$: C, 67.11; H, 9.93. Found C, 67.28; H, 10.11%.

NMR tube reactions

Cp′$_2$CeH and ethoxytrimethylsilane in benzene-d_6. Cp′$_2$CeH was dissolved in C_6D_6 in an NMR tube and a drop of ethoxytrimethylsilane was added. The sample turned red over 2 min, by which time resonances due to Cp′$_2$CeH had disappeared from the ^{1}H NMR spectrum and resonances due to trimethylsilane[18] and Cp′$_2$CeOEt had appeared. Integration of the CMe_3 resonances relative to the solvent residual proton signal indicated that the conversion from Cp′$_2$CeH was quantitative.

Cp′$_2$CeH and propoxytrimethylsilane in benzene-d_6. Cp′$_2$CeH was dissolved in C_6D_6 in an NMR tube and a drop of n-proxytrimethylsilane was added. The sample turned red over 2 min, by which time resonances due to Cp′$_2$CeH had disappeared from the ^{1}H NMR spectrum and resonances due to trimethylsilane and Cp′$_2$CeO-n-Pr had appeared. Integration of the CMe_3 resonances relative to the solvent residual proton signal indicated that the conversion from Cp′$_2$CeH was quantitative.

Cp′$_2$CeH and diethylether (Et_2O) in cyclohexane-d_{12}. Cp′$_2$CeH was dissolved in C_6D_{12} in an NMR tube and a drop of Et_2O was added. The sample was allowed to stand at 19 °C. After 1 d, a new set of paramagnetic resonances due to Cp′$_2$CeOEt had appeared in the ^{1}H NMR spectrum; the ratio of Cp′$_2$CeH to Cp′$_2$CeOEt was 30 : 1. After 9 d, the ratio was 2 : 1, after 36 d 1 : 4 and after 52 d 1 : 20.

Cp′$_2$CeH and dipropylether (n-Pr_2O) in cyclohexane-d_{12}. Cp′$_2$CeH was dissolved in C_6D_{12} in an NMR tube and a drop of n-Pr_2O was added. The sample was heated at 60 °C. After 1 d, resonances due to Cp′$_2$CeO-n-Pr had appeared in the ^{1}H NMR spectrum; the ratio of Cp′$_2$CeH to Cp′$_2$CeO-n-Pr was 33 : 1. After 16 d, the ratio was 5 : 1, after 54 d 1.2 : 1, after 101 d 1 : 2 and after 186 d 1 : 10.

(Cp′-d_{27})$_2$CeD and n-Pr_2O in C_6D_6. Cp′$_2$CeH was dissolved in C_6D_6 and heated at 60 °C for 4 d to perdeuterate the CMe_3 groups. The sample was taken to dryness and the solid residue dissolved in fresh C_6D_6. The sample was heated for an additional 4 d, taken to dryness and the solid residue dissolved in C_6D_6. The ^{2}H NMR spectrum contained $C(CD_3)_3$ resonances consistent with (Cp′-d_{27})$_2$CeD. A drop of n-Pr_2O was added and the sample heated at 60 °C. After 1 d, a broad resonance at δ 3.14 had appeared in the ^{2}H NMR spectrum, and a 1 : 1 : 1 pattern centered at δ 72.52 (J_{CD} = 21 Hz) had appeared in the ^{13}C NMR spectrum δ 0.4 upfield of the signal for the α-carbons of n-Pr_2O, indicating H-for-D exchange. After 16 d, resonances due to (Cp′-d_{27})$_2$CeOPr had appeared in the ^{2}H NMR spectrum; the ratio of (Cp′-d_{27})$_2$CeD to (Cp′-d_{27})$_2$CeOPr was 12 : 1. The spectrum also contained a triplet at δ 3.14 (J_{HD} = 1 Hz) and a multiplet at δ 0.82, indicating that H-for-D exchange had occurred on the α- and γ-carbons of n-Pr_2O; the area ratio of the resonances was 14 : 1. The triplet in the ^{1}H NMR spectrum due to protons on the α-carbons of n-Pr_2O had shifted upfield by δ 0.02 and each peak was split into a 1 : 1 : 1 pattern (J_{HH} = 7 Hz, J_{HD} = 1 Hz). The resonance for the protons on the β-carbons had changed from a coincidental sextet (triplet of quartets) to a quartet (J_{HH} = 7 Hz), and the area ratio of the proton resonances for the α-, β- and γ-carbons was 1 : 19 : 27. A triplet with each peak split into a 1 : 1 : 1 pattern due to γ-CH_2D groups in n-Pr_2O had appeared δ 0.017 upfield of the triplet corresponding to the γ-CH_3 groups. The ^{13}C NMR spectrum contained a multiplet at δ 72.03 (J_{CD} = 21 Hz) for the α-carbons, a singlet for the β-carbons and a singlet plus a 1 : 1 : 1 pattern (J_{CD} = 19 Hz) centered δ 0.29 upfield of the singlet for the γ-carbon resonance. After 186 d, the ratio of (Cp′-d_{27})$_2$CeD to (Cp′-d_{27})$_2$CeOPr in the ^{2}H NMR spectrum was 1 : 1; the area ratio of the resonances corresponding to deuterium on the α- and γ-carbons of n-Pr_2O was 2.5 : 1. The area ratio of the proton resonances for the α-, β- and γ-carbons of n-Pr_2O in the ^{1}H NMR spectrum was 1 : 14 : 18.

Cp′$_2$CeH and dibutylether (n-Bu_2O) in cyclohexane-d_{12}. Cp′$_2$CeH was dissolved in C_6D_{12} in an NMR tube and a drop of n-Bu_2O added. The sample was heated at 60 °C. After 6 d, resonances due to Cp′$_2$CeO-n-Bu had appeared in the ^{1}H NMR spectrum. The ratio of Cp′$_2$CeH to Cp′$_2$CeO-n-Bu was 24 : 1. After 30 d, the ratio was 4 : 1, after 99 d 1 : 1.3

and after 147 d 1 : 4. Gases from the headspace were condensed into a new tube containing C_6D_6 solvent cooled in a liquid nitrogen isopropanol bath. The ^{1}H NMR spectrum contained diamagnetic resonances at δ 1.22 and 0.85, consistent with butane.

(Cp′-d_{27})$_2$CeD and n-Bu$_2$O in C_6D_6. Cp′$_2$CeH was dissolved in C_6D_6 and heated at 60 °C for 4 d to perdeuterate the CMe_3 groups. The sample was taken to dryness and the solid residue dissolved in fresh C_6D_6. The sample was heated for an additional 4 d, taken to dryness and the solid residue dissolved in C_6D_6. The ^{2}H NMR spectrum contained $C(CD_3)_3$ resonances, consistent with (Cp′-d_{27})$_2$CeD. A drop of n-Bu$_2$O was added and the sample heated at 60 °C. After 1 d, a broad resonance at δ 3.21 had appeared in the ^{2}H NMR spectrum, indicating H-for-D exchange on the α-carbon of n-Bu$_2$O. The area ratio of the proton resonances on the α-, β-, γ- and δ-carbons had changed from 2 : 2 : 2 : 3 initially to 1 : 1.2 : 1.2 : 1.8. After 6 d, resonances due to (Cp′-d_{27})$_2$CeOBu had appeared in the ^{2}H NMR spectrum; the ratio of (Cp′-d_{27})$_2$CeD to (Cp′-d_{27})$_2$CeOBu was 13 : 1. The ratio of the proton resonances on the α-, β-, γ- and δ-carbons of n-Bu$_2$O in the ^{1}H NMR spectrum was 1 : 4 : 4 : 6. After 30 d, the ratio of (Cp′-d_{27})$_2$CeD to (Cp′-d_{27})$_2$CeOBu in the ^{2}H NMR spectrum was 5 : 1, and a multiplet had appeared at δ 0.82, indicating H-for-D exchange on the δ-carbons of n-Bu$_2$O, as well as on the α-carbons. The area ratio of the ^{2}H NMR resonances for deuterium on the α- and δ-carbons of n-Bu$_2$O was 30 : 1. The ratio of the proton resonances on the α-, β-, γ- and δ-carbons of n-Bu$_2$O in the ^{1}H NMR spectrum was 1 : 38 : 38 : 56. The ^{13}C NMR spectrum contained a 1 : 3 : 5 : 3 : 1 pattern at δ 70.10 (J_{CD} = 21 Hz) for the α-carbons of n-Bu$_2$O, single resonances for the β- and γ- carbons, and a single resonance plus a 1 : 1 : 1 pattern (J_{CD} = 19 Hz) centered δ 0.30 upfield of the single resonance for the δ-carbon. After 147 d, resonances due to (Cp′-d_{27})$_2$CeD were absent from the ^{2}H NMR spectrum.

Gases from the sample headspace were condensed into a new tube containing C_6D_6 solvent cooled in a liquid nitrogen isopropanol bath. The ^{1}H NMR spectrum contained a multiplet at δ 1.22 and a triplet at δ 0.85, consistent with butane, but in a 1 : 1 area ratio. The ^{2}H NMR spectrum contained a broad singlet at δ 1.28 and a triplet at δ 0.76 in a 1 : 5 area ratio.

The solvent from the original sample was vacuum transferred into a fresh NMR tube. The ^{1}H NMR spectrum contained resonances consistent with n-Bu$_2$O, but the resonance due to protons on the α-carbons had shifted upfield by δ 0.02, and each peak was split into a 1 : 1 : 1 pattern (J_{HH} = 7 Hz, J_{HD} = 1 Hz), consistent with α-CHD groups. The resonance for the protons on the β-carbon appeared as a triplet (J_{HH} = 7 Hz) and the protons on the γ-carbon as a coincidental sextet (triplet of quartets, J_{HH} = 7 Hz). The protons on the δ-carbon appeared as a triplet (J_{HH} = 7 Hz), corresponding to δ-CH_3 groups, and another triplet with each peak split into a 1 : 1 : 1 pattern δ 0.018 upfield, corresponding to δ-CH_2D groups. The area ratio of the α-, β-, γ- and δ-carbon resonances was 1 : 45 : 45 : 59. The ^{2}H NMR spectrum contained a triplet at δ 3.21 (J_{HD} = 1 Hz), corresponding to the deuterons on the α-carbons, and a multiplet at δ 0.83, corresponding to deuterons on the δ-carbons of n-Bu$_2$O; the area ratio of the two signals was 10 : 1. GC-MS analysis of the solution showed the ratio of n-Bu$_2$O-d_2, -d_3, -d_4, -d_5 and d_6 to be 3 : 3 : 32 : 7 : 1.

Computational details

The Stuttgart–Dresden–Bonn relativistic large effective core potential (RECP) was used to represent the inner shells of Ce.[19] The associated basis set[19] augmented by an f-polarization function (α = 1.000) was used to represent the valence orbitals.[20] The atoms C, O and H were represented by an all-electron 6-31G(d,p) basis set.[21] Calculations were carried out at the DFT(B3PW91) level[22] with Gaussian 03.[23] The nature of the extrema (minimum or transition state) were established with analytical frequencies calculations, and the intrinsic reaction coordinate (IRC) was followed to confirm that the transition states connected to the reactants and products. The zero point energy (ZPE) and entropic contribution were estimated within the harmonic potential approximation. The Gibbs free energy, G, was calculated at T = 298.15 K and 1 atm.

Acknowledgements

This work was supported by the Director, Office of Science, Office of Basic Energy Sciences (OBES) of the U.S. Department of Energy (DOE) under Contract no. DE-AC02-05CH11231. A. Y. thanks the Computer Center, CCRT of the CEA for a generous donation of computation time. L. M. and O. E. thank the CNRS and Minister of High Education and Research for funding, and A. Y. thanks the CEA for a PhD fellowship. L. M. is a junior member of the Institut Universitaire de France.

References

1 E. L. Werkema, E. Messines, L. Perrin, L. Maron, O. Eisenstein and R. A. Andersen, *J. Am. Chem. Soc.*, 2005, **127**, 7781.
2 E. L. Werkema, R. A. Andersen, A. Yahia, L. Maron and O. Eisenstein, *Organometallics*, 2009, **28**, 3173.
3 P. L. Watson, *J. Chem. Soc., Chem. Commun.*, 1983, 276.
4 M. E. Thompson, S. M. Baxter, A. R. Bulls, B. J. Berger, M. C. Nolan, B. D. Santarsierio, W. P. Schaefer and J. E. Bercaw, *J. Am. Chem. Soc.*, 1987, **109**, 203.
5 B.-J. Deelman, M. Booji, A. Meetsma, J. H. Teuben, H. Kooijman and A. L. Spek, *Organometallics*, 1995, **14**, 2306.
6 W. J. Evans, T. A. Ulibarri and J. W. Ziller, *Organometallics*, 1991, **10**, 134.
7 E. L. Werkema, L. Maron, O. Eisenstein and R. A. Andersen, *J. Am. Chem. Soc.*, 2007, **129**, 2529 (correction: E. L. Werkema, L. Maron, O. Eisenstein and R. A. Andersen, *J. Am. Chem. Soc.*, 2007, **129**, 6662).
8 E. L. Werkema, R. A. Andersen, L. Maron and O. Eisenstein, *Dalton Trans.*, 2010, DOI: 10.1039/b918103b.
9 S. Niu and M. B. Hall, *Chem. Rev.*, 2000, **100**, 353.
10 K. Ziegler and H.-G. Gellert, *Justus Liebigs Ann. Chem.*, 1950, **567**, 185.
11 A. Maercker and W. Demuth, *Angew. Chem., Int. Ed. Engl.*, 1973, **12**, 75; A. Maercker and W. Demuth, *Justus Liebigs Ann. Chem.*, 1977, 1909; A. Maercker, *Angew. Chem., Int. Ed. Engl.*, 1987, **26**, 972; J. Clayden and S. A. Yasin, *New J. Chem.*, 2002, **26**, 191.
12 K. Tomooka, in *The Chemistry of Organolithium Compounds Part 2*, Patai Series: The Chemistry of Functional Groups, ed. Z. Rappoport and I. Marek, Wiley, New York, 2004, pp. 749–828; M. Braun, in *The Chemistry of Organolithium Compounds Part 2*,

Patai Series: The Chemistry of Functional Groups, ed. Z. Rappoport and I. Marek, Wiley, New York, 2004, pp. 829–900.
13 V. H. Gessner and C. Strohmann, *J. Am. Chem. Soc.*, 2008, **130**, 14412.
14 C. A. Bradley, L. F. Veiros, D. Pun, E. Lobkovsky, I. Keresztes and P. J. Chirik, *J. Am. Chem. Soc.*, 2006, **128**, 16600.
15 W. A. Nugent, D. W. Ovenall and S. J. Holmes, *Organometallics*, 1983, **2**, 161; W. A. Nugent and R. M. Zubyk, *Inorg. Chem.*, 1986, **25**, 4604.
16 L. Maron, E. L. Werkema, L. Perrin, O. Eisenstein and R. A. Andersen, *J. Am. Chem. Soc.*, 2005, **127**, 279.
17 A. Pierce, *Silylation of Organic Compounds: A Technique for Gas-Phase Analysis*, Pierce Chemical Company, Rockford, IL, 1968, pp. 18.
18 M. Okazaki, H. Tobita and H. Ogino, *Chem. Lett.*, 1997, 437.
19 M. Dolg, H. Stoll, A. Savin and H. Preuß, *Theor. Chim. Acta*, 1989, **75**, 173; M. Dolg, H. Stoll and H. Preuß, *Theor. Chim. Acta*, 1993, **85**, 441.
20 L. Maron and O. Eisenstein, *J. Phys. Chem. A*, 2000, **104**, 7140.
21 P. C. Hariharan and J. A. Pople, *Theor. Chim. Acta*, 1973, **28**, 213.
22 J. J. P. Perdew and Y. Wang, *Phys. Rev. B: Condens. Matter*, 1992, **45**, 13244; A. D. Becke, *J. Chem. Phys.*, 1993, **98**, 5648; K. Burke, J. P. Perdew and Y. Wang, in *Electronic Density Functional Theory: Recent Progress and New Directions*, ed. J. F. Dobson, G. Vignale and M. P. Das, Plenum Press, New York, 1998, pp. 81–111.
23 M. J. Frisch, G. W. Trucks, H. B. Schlegel, G. E. Scuseria, M. A. Robb, J. R. Cheeseman, J. A. Montgomery, Jr., T. Vreven, K. N. Kudin, J. C. Burant, J. M. Millam, S. S. Iyengar, J. Tomasi, V. Barone, B. Mennucci, M. Cossi, G. Scalmani, N. Rega, G. A. Petersson, H. Nakatsuji, M. Hada, M. Ehara, K. Toyota, R. Fukuda, J. Hasegawa, M. Ishida, T. Nakajima, Y. Honda, O. Kitao, H. Nakai, M. Klene, X. Li, J. E. Knox, H. P. Hratchian, J. B. Cross, V. Bakken, C. Adamo, J. Jaramillo, R. Gomperts, R. E. Stratmann, O. Yazyev, A. J. Austin, R. Cammi, C. Pomelli, J. Ochterski, P. Y. Ayala, K. Morokuma, G. A. Voth, P. Salvador, J. J. Dannenberg, V. G. Zakrzewski, S. Dapprich, A. D. Daniels, M. C. Strain, O. Farkas, D. K. Malick, A. D. Rabuck, K. Raghavachari, J. B. Foresman, J. V. Ortiz, Q. Cui, A. G. Baboul, S. Clifford, J. Cioslowski, B. B. Stefanov, G. Liu, A. Liashenko, P. Piskorz, I. Komaromi, R. L. Martin, D. J. Fox, T. Keith, M. A. Al-Laham, C. Y. Peng, A. Nanayakkara, M. Challacombe, P. M. W. Gill, B. G. Johnson, W. Chen, M. W. Wong, C. Gonzalez and J. A. Pople, *GAUSSIAN 03 (Revision C.02)*, Gaussian, Inc., Wallingford, CT, 2004.

